



HAL
open science

Persistent Inward Currents in Tibialis Anterior Motoneurons Can Be Reliably Estimated within the Same Session

Thomas Lapole, Ricardo N O Mesquita, Stéphane Baudry, Robin Souron, Callum G Brownstein, Vianney Rozand

► To cite this version:

Thomas Lapole, Ricardo N O Mesquita, Stéphane Baudry, Robin Souron, Callum G Brownstein, et al.. Persistent Inward Currents in Tibialis Anterior Motoneurons Can Be Reliably Estimated within the Same Session. *Journal of Electromyography and Kinesiology*, 2024, 78, pp.102911. 10.2139/ssrn.4749361 . hal-04615539

HAL Id: hal-04615539

<https://nantes-universite.hal.science/hal-04615539>

Submitted on 18 Jun 2024

HAL is a multi-disciplinary open access archive for the deposit and dissemination of scientific research documents, whether they are published or not. The documents may come from teaching and research institutions in France or abroad, or from public or private research centers.

L'archive ouverte pluridisciplinaire **HAL**, est destinée au dépôt et à la diffusion de documents scientifiques de niveau recherche, publiés ou non, émanant des établissements d'enseignement et de recherche français ou étrangers, des laboratoires publics ou privés.

See discussions, stats, and author profiles for this publication at: <https://www.researchgate.net/publication/378952467>

Persistent inward currents in tibialis anterior motoneurons can be reliably estimated within the same session

Preprint · March 2024

DOI: 10.2139/ssrn.4749361

CITATIONS

0

READS

107

7 authors, including:



Thomas Lapole

Université Jean Monnet

114 PUBLICATIONS 1,127 CITATIONS

[SEE PROFILE](#)



Ricardo N. O. Mesquita

Chalmers University of Technology

33 PUBLICATIONS 197 CITATIONS

[SEE PROFILE](#)



Stéphane Baudry

Université Libre de Bruxelles

133 PUBLICATIONS 3,790 CITATIONS

[SEE PROFILE](#)



Robin Souron

University of Nantes

50 PUBLICATIONS 472 CITATIONS

[SEE PROFILE](#)

1 **Persistent inward currents in tibialis anterior motoneurons can be reliably estimated**
2 **within the same session**

3

4 Thomas Lapole^{1*}, Ricardo N. O. Mesquita^{2,3,4*}, Stéphane Baudry⁵, Robin Souron⁶, Eleanor K.
5 O'Brien^{3,7}, Callum G. Brownstein^{8#}, Vianney Rozand^{1,9#}

6

7 ¹ Université Jean Monnet Saint-Etienne, Lyon 1, Université Savoie Mont-Blanc, Laboratoire
8 Interuniversitaire de Biologie de la Motricité, F-42023, SAINT-ETIENNE, FRANCE.

9 ² Department of Electrical Engineering, Chalmers University of Technology, Gothenburg,
10 Sweden.

11 ³ School of Medical and Health Sciences, Edith Cowan University, Perth, Australia

12 ⁴ Neuroscience Research Australia, Sydney, Australia

13 ⁵ Laboratory of Applied Biology, Research Unit in Applied Neurophysiology (LABNeuro),
14 Faculty of Motor Sciences, Université Libre de Bruxelles (ULB), Belgium

15 ⁶ Nantes Université, Mouvement - Interactions - Performance, MIP, UR 4334, F-44000
16 Nantes, France

17 ⁷ Centre for Precision Health, Edith Cowan University, Perth, Western Australia

18 ⁸ Newcastle University, School of Biomedical, Nutritional and Sports Sciences, Newcastle-
19 upon-Tyne, United Kingdom

20 ⁹ INSERM UMR1093-CAPS, Université Bourgogne Franche-Comté, UFR des Sciences du
21 Sport, F-21000 Dijon, France

22

23 * equal first authors

24 # equal senior authors

25

26 **Running title:** Reliability of estimates of PIC contribution to motoneuron firing

27

28 **Corresponding authors**

29 Ricardo N. O. Mesquita

30 Department of Electrical Engineering

31 Chalmers University of Technology

32 Maskingränd 2, Gothenburg, Sweden

33 mesquita@chalmers.se

34 ORCID: 0000-0002-0327-3253

35

36 Thomas LAPOLE

37 Laboratoire Interuniversitaire de Biologie de la Motricité

38 Bâtiment IRMIS ; 10 Rue de la Marandière

39 42270 Saint-Priest-en-Jarez

40 +33 4 77 42 18 91

41 thomas.lapole@univ-st-etienne.fr

42 ORCID: 0000-0002-1477-6614

43 **ABSTRACT**

44 The response of spinal motoneurons to synaptic input greatly depends on the activation of
45 persistent inward currents (PICs), the contribution of which can be estimated through the paired
46 motor unit technique. Yet, the intra-session test-retest reliability of this measurement remains
47 to be fully established. Twenty males performed isometric triangular dorsiflexion contractions
48 to 20 and 50% of maximal torque at baseline and after a 15-min resting period. High-density
49 electromyographic signals (HD-EMG) of the tibialis anterior were recorded with a 64-electrode
50 matrix. HD-EMG signals were decomposed, and motor units tracked across time points to
51 estimate the contribution of PICs to motoneuron firing through quantification of motor unit
52 recruitment-derecruitment hysteresis (ΔF). A good intraclass correlation coefficient (ICC =
53 0.75 [0.63, 0.83]) and a large repeated measures correlation coefficient ($R_{(rm)} = 0.65$ [0.49,
54 0.77]; $p < 0.001$) were found between ΔF values obtained at both time points for 20% MVC
55 ramps. For 50% MVC ramps, a good ICC (0.77 [0.65, 0.85]) and a very large repeated measures
56 correlation coefficient ($R_{(rm)} = 0.73$ [0.63, 0.80]; $p < 0.001$) were observed. Our data suggest that
57 ΔF scores can be reliably investigated in tibialis anterior motor units during both low- and
58 moderate-intensity contractions within a single experimental session.

59

60 **Keywords: neuromodulation, serotonin, noradrenaline, motor neurone, motor neuron**

61 INTRODUCTION

62 Human movement relies on the generation of force by skeletal muscles, a process intricately
63 governed by the interplay between neural and muscular factors. The modulation of muscle force
64 is achieved through modulation of the recruitment of motor units (MUs) and/or increases in
65 their firing frequency. MU firing patterns depend on the synaptic integration occurring at the
66 cell bodies of motoneurons. While voluntary commands from the motor cortex serve as the
67 primary mean of activating alpha-motoneurons, multiple excitatory and inhibitory afferent
68 inputs projecting onto motoneurons influence their activity. Moreover, motoneurons receive
69 serotonergic (Bowker et al., 1981) and noradrenergic (Proudfit and Clark, 1991) inputs from
70 the brainstem. The binding of these neuromodulators to metabotropic receptors initiates
71 intracellular signalling cascades that modulate the properties of voltage-gated channels (i.e.,
72 intrinsic motoneuronal electrical properties) (Powers and Binder, 2001). The most evident
73 neuromodulatory mechanism is the activation of persistent inward currents (PICs) (Heckman
74 et al., 2005; 2009). PICs amplify and prolong the effects of the ionotropic system, introducing
75 non-linearities to the relationship between the net synaptic input to a motoneuron pool and the
76 resulting motor output (Binder et al., 2020).

77

78 The contribution of PICs to motoneuron firing cannot be directly measured in humans.
79 Nonetheless, distinct MU firing patterns have been observed which are likely generated by PICs
80 (Heckman et al., 2009, Heckmann et al., 2005). These firing patterns have been identified *in*
81 *vivo* using decomposition of intramuscular electromyographic signals (e.g., Foley and Kalmar,
82 2019, Marchand-Pauvert et al., 2019, Revill and Fuglevand, 2017) and, more recently, high-
83 density electromyographic signals (HD-EMG) (e.g., Hassan et al., 2021, Khurram et al., 2021,
84 Orssatto et al., 2021). The paired MU technique (Gorassini et al., 2002, Gorassini et al., 1998)
85 allows the estimation of the contribution of PICs to motoneuron firing in humans during

86 submaximal voluntary contractions. During a ramp contraction, the smoothed firing frequency
87 of a lower-threshold control MU is used as a proxy of net synaptic input at the time of
88 recruitment and derecruitment of a higher-threshold MU (test unit). The difference in the
89 smoothed firing rate of the control unit at recruitment and derecruitment of the test unit
90 constitutes the ΔF score (i.e., change in frequency). This method has been validated by
91 intracellular direct PIC measurements in animal models (Bennett et al., 2001) and by computer
92 simulations (Powers and Heckman, 2015). Yet, the test-retest reliability of such measurements
93 has been only scarcely investigated with average scores per participant (Orssatto et al., 2023,
94 Trajano et al., 2020). Using data from all extracted MUs while accounting for the nested
95 structure of the data pertaining to PIC estimates is however imperative to provide a more
96 accurate test of ΔF test-retest variability. Analytical approaches that consider the hierarchical
97 nature of MU data without reducing data to averaged scores within individuals have already
98 been used to assess effects of experimental interventions (e.g., Boccia et al., 2019, Mesquita et
99 al., 2023).

100

101 The aim of the present study was to investigate the intra-session reliability of the contribution
102 of PICs to recruitment-derecruitment firing hysteresis (ΔF) using a linear mixed modelling
103 approach that considers the nestedness typical of these types of data. As secondary objectives,
104 we also investigated reliability of MU recruitment thresholds, derecruitment thresholds and
105 firing rate, and examined whether ΔF scores varied across recruitment thresholds.

106

107

108 **METHODS**

109 **Participants**

110 Twenty male participants volunteered to participate in this study (age: 30 ± 7 yrs, height: 177.9
111 ± 7.0 cm, body mass: 76.5 ± 12.2 kg). Participants were asked to avoid caffeine and alcohol
112 consumption as well as to abstain from strenuous exercise 24 h prior to the testing session.
113 Participants provided written informed consent and this study conformed to the ethical
114 standards set by the Declaration of Helsinki, except for registration in a database. The study
115 was approved by the local research ethics committee (CPP SudEst I; 1408208-2015-A00036-
116 43).

117

118 **Design**

119 Data presented in this study were obtained from a previously published study where we
120 investigated the ongoing and acute effects of local vibration on PICs contribution to
121 motoneuron firing (Lapole et al., 2023). Data collection was performed in a single session, with
122 participants seating on a dynamometer and high-density electromyography (HD-EMG)
123 measurements performed on the tibialis anterior (TA) of the right leg. After a familiarisation
124 period to the experimental procedures, participants performed at least two 3-s maximal
125 isometric voluntary dorsiflexion contractions (MVCs) with a 60-s inter-trial passive rest.
126 Additional MVCs were performed until the difference between the two best trials was less than
127 5%. Participants then performed triangular isometric contractions at baseline (CON-1) and were
128 retested after a 15-min resting period (CON-2) to investigate the reliability of estimates of PIC
129 contribution to motoneuron firing. In each time point, three triangular contractions were
130 performed to both 20 and 50% MVC, with the ascending and descending phase lasting 10 s
131 each (i.e., 2% of $\text{MVC}\cdot\text{s}^{-1}$ and 5% of $\text{MVC}\cdot\text{s}^{-1}$, respectively). Triangular contractions to the
132 same intensity were interspaced by a 30-s rest, and contraction intensities were randomly
133 ordered and separated by 1 min of passive rest.

134

135 **Torque and electromyographic recordings**

136 Dorsiflexion torque was measured during voluntary contractions using a calibrated
137 instrumented pedal (CS1060 300 Nm; FGP Sensors, Les Clayes Sous Bois, France).
138 Participants were seated upright in a custom-built chair with hips at 90° of flexion (0° = neutral
139 position), right knee at 120° of extension (180° = full extension) and right ankle in a neutral
140 position. The foot was securely attached to the pedal with a custom-made hook and loop
141 fastener. Participants were provided with real-time feedback of the torque trace displayed on a
142 large screen. The peak isometric dorsiflexion torque was taken as the highest value during the
143 MVCs and used to set the intensity of the ramp contractions.

144

145 The skin under the electrodes was shaved, abraded with sandpaper, and swabbed with alcohol.
146 One flexible 64-electrode HD-EMG grid was placed on the TA muscle (13 rows x 5 columns).
147 Electrodes had a 1-mm diameter and 8-mm inter-electrode distance (GR08MM1305; OT
148 Bioelettronica, Turin, Italy). The location of the TA was identified through palpation before the
149 array was placed on the muscle belly, with the grid covering most of the TA proximal area (Del
150 Vecchio et al., 2019). The array was attached to the skin by bi-adhesive foam and the skin-to-
151 electrode contact optimised by filling the wells of the adhesive foam with conductive cream
152 (AC Cream, Spes Medica, Genoa, Italy). Strap electrodes dampened with water were placed
153 around the ankle (ground electrode) and wrist (reference electrode). HD-EMG signals were
154 amplified (150x), collected in monopolar mode, through a 16-bit A/D (Quattrocento; OT
155 Bioelettronica, Torino, Italy), band-pass filtered (10-500 Hz) and digitised at a rate of 5120 Hz.
156 EMG signals were recorded and visualised using OTBioLab+ software (version 1.4.2.0, OT
157 Bioelettronica, Torino, Italy) throughout the protocol to ensure acceptable signal quality.

158

159 **Data analysis**

160 *Motor unit identification and tracking*

161 HD-EMG signals and torque recordings were converted from the OT BioLab+ format into
162 MATLAB-compatible data files (Version R2021B, MathWorks, Natick, USA). These files
163 were then processed offline with the DEMUSE software tool (v5.01; The University of
164 Maribor, Slovenia) that relies on the convolutive blind source separation method (Holobar and
165 Zazula, 2007). Band-pass zero-phase (20-500 Hz), zero-phase 2nd order finite impulse response
166 high-pass differential (230 Hz), and notch (50 Hz and their higher harmonics) filters were
167 applied in DEMUSE. For each subject, the three channels with the lowest signal-to-noise ratio
168 were automatically removed to optimise decomposition, and 50 sequential decomposition runs
169 were conducted in each ramp contraction independently. For each time point and contraction
170 intensity (20 and 50%), only the best ramp contraction was retained for analysis. Ramps were
171 selected by the experimenter based on smoothness and adherence to the torque template, as well
172 as the number of identified MUs.

173

174 For each contraction intensity, the selected ramps were concatenated and the same MUs were
175 tentatively tracked over the different time points. MU duplicates were removed and spike trains
176 visually inspected and manually edited by a trained investigator (Del Vecchio et al., 2020).
177 After editing, only MUs that presented a global pulse-to-noise ratio greater than 30 dB were
178 retained for further analysis (Holobar et al., 2014).

179

180 *Extraction of motor unit firing characteristics*

181 After carefully editing the spike trains, firing events were converted into instantaneous firing
182 rates and smoothed using a 5th order polynomial function, with additional MATLAB scripts
183 and functions. All polynomials were visually inspected and if edge effects were observed at
184 MU recruitment or derecruitment (i.e., a clear mismatch between the change in the smoothed

185 and instantaneous firing rate), the MU from that specific trial was not included in further
186 analyses. MU maximal firing rate was considered as the maximal value obtained from the
187 polynomial curve (i.e., smoothed peak firing rate). Recruitment and derecruitment thresholds
188 were also computed as the torque level (% MVC) at the time when the MU started and stopped
189 firing action potentials, respectively.

190
191 We then used the paired MU technique (Gorassini et al., 2002, Gorassini et al., 1998) to estimate
192 the contribution of PICs to TA motoneuron firing (see Lapole et al. (2023), Figure 1). This
193 technique quantifies MU recruitment-derecruitment hysteresis (i.e., ΔF). Lower-threshold MUs
194 (i.e., control units) were paired with higher-threshold MUs (i.e., test units), with the smoothed
195 firing frequency of control units being used as an estimate of changes in the net synaptic input.
196 In each MU pair, the hysteresis of the test unit was quantified by calculating the difference
197 between the smoothed firing rates of the control unit at recruitment and derecruitment of the
198 test unit, which constitutes the ΔF (change in frequency) score (Gorassini et al., 2002). A MU
199 pair was only considered for analysis if the test unit was derecruited before the control unit.
200 Furthermore, criteria were used to test the assumption that the control unit was a suitable proxy
201 for net synaptic input. Pairs were included if rate-to-rate Pearson's correlation coefficients
202 between the smoothed firing rate polynomials of the test and control units (calculated from
203 5120 data points per second on Excel, Version 2019, Microsoft Corporation, USA) were $r > 0.7$
204 (Stephenson and Maluf, 2011), so as to ensure that control and test MUs likely shared a common
205 synaptic drive. The first 500 ms of the test unit were excluded from the correlation analysis to
206 minimise contamination of a non-linear firing rate acceleration at the time of recruitment
207 (Mottram et al., 2009). Moreover, only pairs with a recruitment time difference greater than 1
208 s were considered to meet the assumption that PICs in the control unit were fully activated when
209 the test unit was recruited, avoiding the contamination of the aforementioned non-linear firing

210 rate acceleration (Hassan et al., 2020). Finally, a saturation criterion was used, excluding pairs
211 in which the control unit did not increase its firing rate more than 0.5 Hz after the recruitment
212 of the test unit, as the control unit would not be sensitive to changes in synaptic drive
213 (Stephenson and Maluf, 2011).

214
215 The quantification of the variables that were needed for the ΔF calculation, as well as the
216 identification of suitable pairs and calculation of ΔF values were conducted in Excel (Version
217 2019, Microsoft Corporation, Redmond, USA). Data were compared between CON-1 and
218 CON-2 to investigate the reliability of ΔF measurements. Only pairs identified at the two time
219 points were used for ΔF calculation. Importantly, ΔF scores were calculated for individual test
220 units as the average value obtained when the units were paired with multiple suitable control
221 units, as previously conducted (Trajano et al., 2020).

222

223 **Statistical analysis**

224 Analyses of MU variables were conducted in R (version 4.0.5), using RStudio environment
225 (version 1.4.1106). Reliability analyses from the entire set of MUs were conducted by
226 computing intraclass correlation coefficients (ICCs) and repeated measures correlations
227 coefficients for ΔF scores, recruitment thresholds, derecruitment thresholds, and peak smoothed
228 firing rates. To calculate ICCs, a linear mixed-effect model with random intercepts was
229 computed (*lmerTest* package; Bates et al. (2015)). The model included a fixed intercept term
230 and 'motor unit' nested within 'participant' were specified as random factors ($Variable \sim 1 +$
231 $(1|Participant/Motor_unit)$). ICCs were calculated by dividing the variance of interest by the
232 total variance of the model (Nakagawa et al., 2017). Confidence intervals (95%) for ICCs were
233 calculated by bootstrapping. Values between 0 and 0.50 were considered as poor, 0.50 and 0.75
234 as moderate, 0.75 and 0.90 as good, and > 0.90 as excellent (Koo and Li, 2016). Repeated-

235 measures correlations coefficients ($R_{(rm)}$) were also computed between CON-1 and CON-2
236 values using the *rmcorr* package (Bakdash and Marusich, 2017). Correlation magnitude was
237 interpreted based on Cohen's criteria (Cohen, 2013): trivial, $R_{(rm)} < 0.1$; weak, $R_{(rm)} = 0.1-0.3$;
238 moderate, $R_{(rm)} = 0.3-0.5$; large, $R_{(rm)} = 0.5-0.7$; very large, $R_{(rm)} = 0.7-0.9$; and nearly perfect,
239 $R_{(rm)} > 0.9$. Furthermore, average scores per participant and per time point were also computed
240 to calculate coefficients of variation (CVs) as the ratio between the standard deviation and the
241 mean of individual measurements. This process was repeated for each participant, resulting in
242 individual CV values for each MU variable during both 20% and 50% ramp contractions. To
243 obtain an aggregated measure of the CV across participants, the mean of these individual CVs
244 was then calculated for each parameter (Knutson et al., 1994).

245

246 Separate linear mixed-effects models were also used to examine whether ΔF scores, MU
247 recruitment thresholds, MU derecruitment thresholds, and peak smoothed firing rates were
248 significantly different between CON-1 and CON-2 (Boccia et al., 2019). Variables were
249 analysed with a random intercept (parallel slopes) model using 'time point' as a fixed effect,
250 and 'motor unit' nested in 'participant' as random effects (*Variable ~ time_point + (1 |*
251 *Participant/Motor_Unit)*). Residuals were plotted against fitted values to assess whether
252 variance was consistent across the fitted range and Q-Q plot inspection was used to assess the
253 assumption of normality of residuals. Estimated marginal means (with 95% confidence
254 intervals [CI]) were quantified (*emmeans* package; Lenth and Lenth (2018)). Significance was
255 set at $p < 0.05$.

256

257 Finally, repeated measures correlations were also computed (*rmcorr* package; Bakdash and
258 Marusich (2017)) to investigate an association between the magnitude of ΔF and MU
259 recruitment threshold during both time points.

260 **RESULTS**

261 **Motor unit identification**

262 MUs could not be identified in two out of 20 participants. Additionally, MUs could not be
263 identified during 20% MVC ramps in two additional participants, and during 50% MVC ramps
264 in two others. Therefore, data presented below are from 16 participants for both 20 and 50%
265 MVC ramps. A total of 260 (16.2 ± 9.4 per participant) and 256 (15.8 ± 8.6 per participant)
266 MUs were tracked during 20 and 50% MVC ramps, respectively, across both CON-1 and CON-
267 2. Of those MUs, a total of 27 (1.7 ± 2.0 per participant) and 20 (1.3 ± 1.5 per participant) MUs
268 exhibited edge effects and were excluded from analysis.

269

270 **Reliability of ΔF measurements**

271 A total of 84 test units (5.6 ± 3.6 per participant) and 468 pairs (31.2 ± 44.9 per participant)
272 were successfully tracked during both ramp contractions (CON-1 and CON-2) performed at
273 20% MVC. In one participant, we were unable to track any pairs between CON-1 and CON-2
274 ($n = 15$). During 50% MVC ramps, we successfully tracked 141 test units (8.4 ± 5.9 per
275 participant) and 794 pairs (55.8 ± 68.9 per participant) during both contractions (CON-1 and
276 CON-2).

277

278 ICCs of ΔF values obtained at CON-1 and CON-2 were good with values of 0.75 [0.63, 0.83]
279 and 0.77 [0.65, 0.85] for 20% and 50% ramps, respectively. There was also a large repeated
280 measures correlation for 20% MVC ramps ($R_{(rm)} = 0.65$ [0.49, 0.77]; $p < 0.001$; Figure 1A), and
281 a very large repeated measures correlation for 50% MVC ramps ($R_{(rm)} = 0.73$ [0.63, 0.80];
282 $p < 0.001$; Figure 1B). CVs were $13.4 \pm 10.0\%$ and $15.9 \pm 8.4\%$ for 20% and 50% MVC ramps,
283 respectively.

284

285 There was no significant change of ΔF from CON-1 to CON-2 for both 20% ($F_{(1,83)} = 3.0$;
286 $p=0.08$) and 50% MVC ramps ($F_{(1,140)} = 0.07$; $p=0.80$) (Table 1). In 20% ramps, a mean
287 difference of +0.2 Hz [-0.03, 0.4] was observed. The mean difference in 50% ramps was +0.03
288 Hz [-0.2, 0.3].

289

290 **Reliability of motor units' thresholds and firing rate**

291 When considering recruitment threshold values obtained in CON-1 and CON-2 for all the
292 identified MUs, ICC was good (i.e., 0.86 [0.82, 0.89]) for 20% MVC ramps and excellent (i.e.,
293 0.95 [0.94, 0.96]) for 50% MVC ramps. Moreover, we observed a nearly perfect repeated-
294 measures correlation between recruitment threshold values obtained in CON-1 and CON-2 for
295 both 20% ($R_{(rm)} = 0.93$ [0.91, 0.95]; $p<0.001$) and 50% MVC ramps ($R_{(rm)} = 0.98$ [0.97, 0.98];
296 $p<0.001$). Yet, recruitment threshold values were significantly decreased from CON-1 to CON-
297 2 for 20% ($F_{(1,233)} = 16.8$; $p<0.001$) and were significantly increased from CON-1 to CON-2 for
298 50% MVC ramp contractions ($F_{(1,233)} = 20.0$; $p<0.001$) (Table 1). Estimated mean differences
299 from CON-1 to CON-2 were -0.6% MVC [-0.3, -0.9] and +1.1% MVC [0.6, 1.6], respectively.
300 CVs were $31.3 \pm 15.1\%$ and $16.6 \pm 15.6\%$ for 20% and 50% MVC ramps, respectively.

301

302 Similar results were observed for derecruitment threshold (Table 1). ICCs were 0.84 [0.80,
303 0.87] and 0.96 [0.94, 0.97] for 20 and 50% MVC ramps, suggesting good and excellent
304 reliability, respectively. Moreover, nearly perfect repeated-measures correlation coefficients
305 were observed between values obtained in CON-1 and CON-2 for both 20% ($R_{(rm)} = 0.92$ [0.90,
306 0.94]; $p<0.001$) and 50% MVC ramps ($R_{(rm)} = 0.98$ [0.97, 0.98]; $p < 0.001$). However, values
307 were significantly increased between the two time points for both 20% ($F_{(1,233)} = 4.7$; $p=0.03$)
308 and 50% MVC ramp contractions ($F_{(1,233)} = 27.2$; $p<0.001$). Estimated mean differences from

309 CON-1 to CON-2 were +0.3% MVC [0.03, 0.5] and +1.2% MVC [0.7, 1.6], respectively. CVs
310 were $19.8 \pm 8.1\%$ and $12.0 \pm 10.5\%$ for 20 and 50% MVC ramps, respectively.

311
312 For smoothed peak firing rate (Table 1), ICCs were excellent (i.e., 0.92 [0.85, 0.94]) and good
313 (i.e., 0.83 [0.73, 0.89]) for 20 and 50% MVC ramps, respectively. There was a nearly perfect
314 correlation between values obtained in CON-1 and CON-2 for 20% MVC ramps ($R_{(rm)} = 0.92$
315 [0.89, 0.94]; $p < 0.001$) while it was very large for 50% MVC ramps ($R_{(rm)} = 0.88$ [0.84, 0.91];
316 $p < 0.001$). Values were significantly decreased between the two time points for 50% MVC
317 contractions ($F_{(1,233)} = 15.7$; $p < 0.001$) with an estimated mean difference from CON-1 to CON-2
318 of -0.4 Hz [-0.2, -0.7]. No difference was observed for 20% MVC contractions ($F_{(1,233)} = 0.3$; -
319 0.04 Hz [-0.2, 0.09]; $p = 0.56$). CVs were $3.6 \pm 2.0\%$ and $5.0 \pm 4.3\%$ for 20% and 50% MVC
320 ramps, respectively.

321

322 **Correlations between recruitment threshold of test units and ΔF values**

323 In 20% MVC ramps, ΔF was moderately associated with the recruitment threshold of test units
324 in both CON-1 ($R_{(rm)} = 0.42$ [0.21, 0.60]; $p < 0.001$) and CON-2 ($R_{(rm)} = 0.47$ [0.26, 0.64];
325 $p < 0.001$) (Figure 2). In 50% MVC ramps, a small correlation was observed in CON-2 ($R_{(rm)} =$
326 0.22 [0.05, 0.38]; $p = 0.01$) but not in CON-1 ($R_{(rm)} = 0.05$ [-0.13, 0.22]; $p = 0.61$) (Figure 2).

327

328 **DISCUSSION**

329 Our results showed good ICC values and large to very large repeated-measures correlations
330 between ΔF values obtained at two time points separated by 15 min of rest. Similarly, good to
331 excellent ICC values and very large to nearly perfect correlations were observed for MU firing
332 rate and both recruitment and derecruitment thresholds, despite a significant difference between

333 the two time points. These results indicate that ΔF can be reliably investigated in TA
334 motoneurons during both low- and moderate-intensity contractions. These findings hold
335 particular importance given that (1) ΔF scores from a single contraction are often used in
336 comparisons between control and experimental conditions (e.g., Goodlich et al., 2023a,
337 Orssatto et al., 2022), and (2) decomposition of HD-EMG signals from the tibialis anterior are
338 commonly used to compute ΔF scores (e.g., Beauchamp et al., 2023, Goodlich et al., 2023a,
339 Goreau et al., 2024, Jenz et al., 2023, Orssatto et al., 2022, Trajano et al., 2023).

340

341 Few studies previously investigated intra-session (Goodlich et al., 2023b, Hoshizaki et al.,
342 2020, Martinez-Valdes et al., 2016, Trajano et al., 2020) and inter-session (e.g., Colquhoun et
343 al., 2018, Goodlich et al., 2023b, Hoshizaki et al., 2020, Martinez-Valdes et al., 2017) reliability
344 of MU variables computed from HD-EMG decomposition. To the best of our knowledge, only
345 two studies have examined intra-session (Trajano et al., 2020) and inter-session (Orssatto et al.,
346 2023) reliability outcomes (i.e., ICC) of ΔF measurements. In an effort to address limitations
347 of the statistical approaches employed in previous MU studies, our reliability analyses utilised
348 the entire set of computed scores (i.e., rather than an average score per participant), thereby
349 enhancing statistical power while taking into consideration the nested structure of the data (i.e.,
350 multiple MUs per participant) (Galbraith et al., 2010, Moen et al., 2016). This is particularly
351 crucial given that MU firing values are highly correlated within a participant, even across
352 testing days (Tenan et al., 2014), and given the significant variability in the number of extracted
353 MUs among participants (Oliveira et al., 2022). To this end, ICCs, calculated as the between-
354 observation variance as a proportion of the total variance from a mixed model approach were
355 calculated (Nakagawa et al., 2017), and repeated-measures correlations (Bakdash and
356 Marusich, 2017) used for the examination of reliability levels. Moreover, CV values, a widely
357 accepted reliability index within the scientific community, were reported. However, a note of

358 caution is due here, as average scores per participant were used to compute CVs, adhering to a
359 reduced data approach to maintain the assumption of independence between observations.

360

361 As ΔF computation depends on MU firing characteristics, intra-session reliability of other
362 variables was also calculated. Recruitment and derecruitment thresholds and smoothed firing
363 rate obtained in CON-1 and CON-2 presented good to excellent ICC values, and repeated-
364 measures correlations were very large to nearly perfect for both low (i.e., 20% MVC) and
365 moderate (i.e., 50% MVC) triangular ramp contractions. To the best of our knowledge, this is
366 the first study to report reliability indices of threshold values. Moreover, the reliability levels
367 for smoothed peak firing rate in this study align consistently with previous research, which has
368 demonstrated good to excellent intra-session reliability (Hoshizaki et al., 2020, Martinez-
369 Valdes et al., 2016, Trajano et al., 2020). Despite good reliability, our results showed significant
370 differences between threshold and firing rates values recorded at both control time points,
371 except for smoothed peak firing rate during 20% MVC ramps. The observed differences in MU
372 characteristics between contractions of similar characteristics is not unexpected considering
373 that the same task can be accomplished by multiple combinations of muscle activation patterns,
374 i.e., muscle redundancy (Latash et al., 2010), leading to variability in the recruitment and firing
375 patterns of MUs. This inherent variability may explain the small estimated mean differences
376 between time points, a phenomenon also noted in prior studies (Martinez-Valdes et al., 2016,
377 Trajano et al., 2020).

378

379 Interestingly, while there were some significant differences in MUs' thresholds as well as
380 smoothed peak firing rate, such differences were not observed for ΔF , which exhibited
381 relatively low estimated mean differences between control time points (+0.2 Hz and +0.03 Hz
382 for 20% and 50% MVC ramps, respectively). Accordingly, our reliability examinations

383 revealed good ICC values, a large repeated-measures correlation between CON-1 and CON-2
384 ΔF values during 20% MVC ramps, and very large during 50% MVC ramps. Although different
385 statistical approaches were used, these results for the TA muscle are consistent with the high
386 ICC values previously reported for the soleus and gastrocnemius medialis muscles in an intra-
387 session design (Trajano et al., 2020), as well as for the TA in an inter-session examination
388 (Orssatto et al., 2023). Collectively, these outcomes suggest that estimates of PICs can be
389 reliably investigated through the paired MU technique during both low- and moderate-intensity
390 contractions. This holds significance as ΔF as small as 0.58 Hz have recently been associated
391 with large increases in peak firing rates and with moderate to very large improvements in motor
392 function (Orssatto et al., 2023). It is important to acknowledge, however, that our focus was
393 only on the intra-session reliability of ΔF scores. Future studies should then investigate its inter-
394 session reliability while taking advantage of the large samples of MU data provided by HD-
395 EMG decomposition and concurrently considering the nested structure of these large datasets.
396

397 Finally, we provide evidence that ΔF scores may depend on the recruitment threshold of the
398 MU. Correlations between ΔF scores and the recruitment threshold of test units was only
399 evident (i.e., moderate correlation) in 20% MVC ramps (Figures 2A and 2B), with this
400 correlation being either small or absent for 50% MVC ramps (Figures 2C and 2D). Our findings
401 partly suggest that there is a tendency for greater magnitudes of suprathreshold PICs in
402 motoneurons of larger sizes (Henneman, 1957). This possibility is consistent with animal
403 studies (Huh et al., 2017, Lee and Heckman, 1998, Sharples and Miles, 2021), one human study
404 in which MUs were identified from intramuscular recordings (Stephenson and Maluf, 2011),
405 and another human study in which multiple MUs were identified from HD-EMG signals
406 (Beauchamp et al., 2023). However, it is contrary to three studies of multiple human MUs
407 identified from HD-EMG signals (Afsharipour et al., 2020, Mesquita et al., 2023, Mesquita et

408 al., 2022) and some animal evidence (Li et al., 2004). Future studies should continue to explore
409 whether contribution of PICs to motoneuron firing varies with human motoneuron size and
410 respective implications in motor output.

411

412 **CONCLUSION**

413 The present study showed that the contribution of PICs to motoneuron firing (ΔF) can be
414 reliably investigated within the same experimental session in TA motoneurons during both low-
415 and moderate-intensity contractions. Moreover, our data suggests that motoneurons recruited
416 at low levels of force may exhibit less recruitment-derecruitment hysteresis in triangular
417 contractions, in comparison with motoneurons recruited at higher levels of force.

418

419

420 **ADDITIONAL INFORMATION SECTION**

421

422 **Competing interests**

423 There are no competing interests, financial or otherwise to report regarding this manuscript.

424

425 **Authors contribution**

426 T.L., RNO.M, CG.B and V.R. conceived and designed the research; T.L., CG.B and V.R.
427 performed experiments; T.L., RNO.M, CG.B, V.R. and EK O. analysed data; T.L., RNO.M,
428 S.B. R.S., CG.B and V.R. interpreted the results of experiments; T.L. and RNO. prepared
429 figures; T.L. and RNO.M drafted the manuscript; all authors edited and revised the manuscript.

430 All authors approved the final version of the manuscript and agreed to be accountable for all
431 aspects of the work in ensuring that questions related to the accuracy or integrity of any part of

432 the work are appropriately investigated and resolved. All persons designated as authors qualify
433 for authorship, and all those who qualify for authorship are listed.

434

435 **Data availability statement**

436 Individual data that support the findings of this study are available from the corresponding
437 author on request.

438

439 **Funding**

440 This work was funded by the Jean Monnet University of Saint-Etienne through funding of the
441 high-density electromyography device, allowing a 6-month teaching discharge to T.L. to work
442 on this study.

443

444 **Acknowledgments**

445 We thank Franck Le Mat for his assistance on statistical analysis.

446 **REFERENCES**

- 447 Afsharipour B, Manzur N, Duchcherer J, Fenrich KF, Thompson CK, Negro F, Quinlan KA, Bennett DJ,
448 Gorassini MA. Estimation of self-sustained activity produced by persistent inward currents using firing
449 rate profiles of multiple motor units in humans. *J Neurophysiol.* 2020;124(1):63-85.
- 450 Bakdash JZ, Marusich LR. Repeated Measures Correlation. *Frontiers in psychology.* 2017;8:456.
- 451 Bates D, Mächler M, Bolker B, Walker S. Fitting Linear Mixed-Effects Models Using lme4. *Journal of*
452 *Statistical Software.* 2015;67(1).
- 453 Beauchamp JA, Pearcey GEP, Khurram OU, Chardon M, Wang YC, Powers RK, Dewald JPA, Heckman CJ.
454 A geometric approach to quantifying the neuromodulatory effects of persistent inward currents on
455 individual motor unit discharge patterns. *Journal of neural engineering.* 2023;20(1).
- 456 Bennett DJ, Li Y, Harvey PJ, Gorassini M. Evidence for plateau potentials in tail motoneurons of awake
457 chronic spinal rats with spasticity. *J Neurophysiol.* 2001;86(4):1972-82.
- 458 Binder MD, Powers RK, Heckman CJ. Nonlinear Input-Output Functions of Motoneurons. *Physiology.*
459 2020;35(1):31-9.
- 460 Boccia G, Martinez-Valdes E, Negro F, Rainoldi A, Falla D. Motor unit discharge rate and the estimated
461 synaptic input to the vasti muscles is higher in open compared with closed kinetic chain exercise.
462 *Journal of applied physiology.* 2019;127(4):950-8.
- 463 Bowker RM, Westlund KN, Coulter JD. Serotonergic projections to the spinal cord from the midbrain
464 in the rat: an immunocytochemical and retrograde transport study. *Neurosci Lett.* 1981;24(3):221-6.
- 465 Cohen J. *Statistical Power Analysis for the Behavioral Sciences.* 2nd Edition 2013.
- 466 Colquhoun RJ, Tomko PM, Magrini MA, Muddle TWD, Jenkins NDM. The influence of input excitation
467 on the inter- and intra-day reliability of the motor unit firing rate versus recruitment threshold
468 relationship. *J Neurophysiol.* 2018;120(6):3131-9.
- 469 Del Vecchio A, Holobar A, Falla D, Felici F, Enoka RM, Farina D. Tutorial: Analysis of motor unit discharge
470 characteristics from high-density surface EMG signals. *J Electromyogr Kinesiol.* 2020;53:102426.

471 Del Vecchio A, Negro F, Holobar A, Casolo A, Folland JP, Felici F, Farina D. You are as fast as your motor
472 neurons: speed of recruitment and maximal discharge of motor neurons determine the maximal rate
473 of force development in humans. *J Physiol.* 2019;597(9):2445-56.

474 Foley RCA, Kalmar JM. Estimates of persistent inward current in human motor neurons during postural
475 sway. *J Neurophysiol.* 2019;122(5):2095-110.

476 Galbraith S, Daniel JA, Vissel B. A study of clustered data and approaches to its analysis. *J Neurosci.*
477 2010;30(32):10601-8.

478 Goodlich BI, Del Vecchio A, Horan SA, Kavanagh JJ. Blockade of 5-HT₂ receptors suppresses motor unit
479 firing and estimates of persistent inward currents during voluntary muscle contraction in humans. *The*
480 *Journal of Physiology.* 2023a;601(6):1121-38.

481 Goodlich BI, Del Vecchio A, Kavanagh JJ. Motor unit tracking using blind source separation filters and
482 waveform cross-correlations: reliability under physiological and pharmacological conditions. *Journal*
483 *of applied physiology.* 2023b;135(2):362-74.

484 Gorassini M, Yang JF, Siu M, Bennett DJ. Intrinsic activation of human motoneurons: possible
485 contribution to motor unit excitation. *J Neurophysiol.* 2002;87(4):1850-8.

486 Gorassini MA, Bennett DJ, Yang JF. Self-sustained firing of human motor units. *Neurosci Lett.*
487 1998;247(1):13-6.

488 Goreau V, Hug F, Jannou A, DERNONCOURT F, CROUZIER M, CATTAGNI T. Estimates of persistent inward
489 currents in lower limb muscles are not different between inactive, resistance-trained, and endurance-
490 trained young males. *J Neurophysiol.* 2024;131(2):166-75.

491 Hassan A, Thompson CK, Negro F, Cummings M, Powers RK, Heckman CJ, Dewald JPA, McPherson LM.
492 Impact of parameter selection on estimates of motoneuron excitability using paired motor unit
493 analysis. *Journal of neural engineering.* 2020;17(1):016063.

494 Hassan AS, Fajardo ME, Cummings M, McPherson LM, Negro F, Dewald JPA, Heckman CJ, Pearcey GEP.
495 Estimates of persistent inward currents are reduced in upper limb motor units of older adults. *J Physiol.*
496 2021;599(21):4865-82.

497 Heckman CJ, Mottram C, Quinlan K, Theiss R, Schuster J. Motoneuron excitability: the importance of
498 neuromodulatory inputs. *Clin Neurophysiol.* 2009;120(12):2040-54.

499 Heckmann CJ, Gorassini MA, Bennett DJ. Persistent inward currents in motoneuron dendrites:
500 implications for motor output. *Muscle Nerve.* 2005;31(2):135-56.

501 Henneman E. Relation between size of neurons and their susceptibility to discharge. *Science.*
502 1957;126(3287):1345-7.

503 Holobar A, Minetto MA, Farina D. Accurate identification of motor unit discharge patterns from high-
504 density surface EMG and validation with a novel signal-based performance metric. *Journal of neural*
505 *engineering.* 2014;11(1):016008.

506 Holobar A, Zazula D. Multichannel Blind Source Separation Using Convolution Kernel Compensation.
507 *IEEE Transactions on Signal Processing.* 2007;55(9):4487-96.

508 Hoshizaki T, Clancy EA, Gabriel DA, Green LA. The reliability of surface EMG derived motor unit
509 variables. *J Electromyogr Kinesiol.* 2020;52:102419.

510 Huh S, Siripuram R, Lee RH, Turkin VV, O'Neill D, Hamm TM, Heckman CJ, Manuel M. PICs in
511 motoneurons do not scale with the size of the animal: a possible mechanism for faster speed of muscle
512 contraction in smaller species. *J Neurophysiol.* 2017;118(1):93-102.

513 Jenz ST, Beauchamp JA, Gomes MM, Negro F, Heckman CJ, Pearcey GEP. Estimates of persistent inward
514 currents in lower limb motoneurons are larger in females than in males. *J Neurophysiol.*
515 2023;129(6):1322-33.

516 Khurram OU, Negro F, Heckman CJ, Thompson CK. Estimates of persistent inward currents in tibialis
517 anterior motor units during standing ramped contraction tasks in humans. *J Neurophysiol.*
518 2021;126(1):264-74.

519 Knutson LM, Soderberg GL, Ballantyne BT, Clarke WR. A study of various normalization procedures for
520 within day electromyographic data. *Journal of Electromyography and Kinesiology.* 1994;4(1):47-59.

521 Koo TK, Li MY. A Guideline of Selecting and Reporting Intraclass Correlation Coefficients for Reliability
522 Research. *Journal of chiropractic medicine.* 2016;15(2):155-63.

523 Lapole T, Mesquita RNO, Baudry S, Souron R, Brownstein CG, Rozand V. Can local vibration alter the
524 contribution of persistent inward currents to human motoneuron firing? *J Physiol.* 2023;601(8):1467-
525 82.

526 Latash ML, Levin MF, Scholz JP, Schoner G. Motor control theories and their applications. *Medicina*
527 (Kaunas). 2010;46(6):382-92.

528 Lee RH, Heckman CJ. Bistability in spinal motoneurons in vivo: systematic variations in rhythmic firing
529 patterns. *J Neurophysiol.* 1998;80(2):572-82.

530 Lenth R, Lenth MR. Package 'lsmeans'. *The American Statistician.* 2018;34(4):216-21.

531 Li Y, Gorassini MA, Bennett DJ. Role of persistent sodium and calcium currents in motoneuron firing
532 and spasticity in chronic spinal rats. *J Neurophysiol.* 2004;91(2):767-83.

533 Marchand-Pauvert V, Peyre I, Lackmy-Vallee A, Querin G, Bede P, Lacomblez L, Debs R, Pradat PF.
534 Absence of hyperexcitability of spinal motoneurons in patients with amyotrophic lateral sclerosis. *J*
535 *Physiol.* 2019;597(22):5445-67.

536 Martinez-Valdes E, Laine CM, Falla D, Mayer F, Farina D. High-density surface electromyography
537 provides reliable estimates of motor unit behavior. *Clin Neurophysiol.* 2016;127(6):2534-41.

538 Martinez-Valdes E, Negro F, Laine CM, Falla D, Mayer F, Farina D. Tracking motor units longitudinally
539 across experimental sessions with high-density surface electromyography. *J Physiol.*
540 2017;595(5):1479-96.

541 Mesquita RNO, Taylor JL, Trajano GS, Holobar A, Goncalves BAM, Blazeovich AJ. Effects of jaw clenching
542 and mental stress on persistent inward currents estimated by two different methods. *The European*
543 *journal of neuroscience.* 2023;58(9):4011-33.

544 Mesquita RNO, Taylor JL, Trajano GS, Skarabot J, Holobar A, Goncalves BAM, Blazeovich AJ. Effects of
545 reciprocal inhibition and whole-body relaxation on persistent inward currents estimated by two
546 different methods. *J Physiol.* 2022;600(11):2765-87.

547 Moen EL, Fricano-Kugler CJ, Luikart BW, O'Malley AJ. Analyzing Clustered Data: Why and How to
548 Account for Multiple Observations Nested within a Study Participant? *PLoS One.* 2016;11(1):e0146721.

549 Mottram CJ, Suresh NL, Heckman CJ, Gorassini MA, Rymer WZ. Origins of abnormal excitability in
550 biceps brachii motoneurons of spastic-paretic stroke survivors. *J Neurophysiol.* 2009;102(4):2026-38.

551 Nakagawa S, Johnson PCD, Schielzeth H. The coefficient of determination R^2 and intra-class
552 correlation coefficient from generalized linear mixed-effects models revisited and expanded. *Journal*
553 *of the Royal Society, Interface / the Royal Society.* 2017;14(134).

554 Oliveira DS, Casolo A, Balshaw TG, Maeo S, Lanza MB, Martin NRW, Maffulli N, Kinfe TM, Eskofier BM,
555 Folland JP, Farina D, Del Vecchio A. Neural decoding from surface high-density EMG signals: influence
556 of anatomy and synchronization on the number of identified motor units. *Journal of neural*
557 *engineering.* 2022;19(4).

558 Orssatto LBR, Fernandes GL, Blazeovich AJ, Trajano GS. Facilitation-inhibition control of motor neuronal
559 persistent inward currents in young and older adults. *J Physiol.* 2022;600(23):5101-17.

560 Orssatto LBR, Mackay K, Shield AJ, Sakugawa RL, Blazeovich AJ, Trajano GS. Estimates of persistent
561 inward currents increase with the level of voluntary drive in low-threshold motor units of plantar flexor
562 muscles. *J Neurophysiol.* 2021;125(5):1746-54.

563 Orssatto LBR, Rodrigues P, Mackay K, Blazeovich AJ, Borg DN, Souza TR, Sakugawa RL, Shield AJ, Trajano
564 GS. Intrinsic motor neuron excitability is increased after resistance training in older adults. *J*
565 *Neurophysiol.* 2023;129(3):635-50.

566 Powers RK, Binder MD. Input-output functions of mammalian motoneurons. *Rev Physiol Biochem*
567 *Pharmacol.* 2001;143:137-263.

568 Powers RK, Heckman CJ. Contribution of intrinsic motoneuron properties to discharge hysteresis and
569 its estimation based on paired motor unit recordings: a simulation study. *J Neurophysiol.*
570 2015;114(1):184-98.

571 Proudfit HK, Clark FM. The projections of locus coeruleus neurons to the spinal cord. *Prog Brain Res.*
572 1991;88:123-41.

573 Revill AL, Fuglevand AJ. Inhibition linearizes firing rate responses in human motor units: implications
574 for the role of persistent inward currents. *J Physiol.* 2017;595(1):179-91.

575 Sharples SA, Miles GB. Maturation of persistent and hyperpolarization-activated inward currents
576 shapes the differential activation of motoneuron subtypes during postnatal development. *Elife*.
577 2021;10.

578 Stephenson JL, Maluf KS. Dependence of the paired motor unit analysis on motor unit discharge
579 characteristics in the human tibialis anterior muscle. *Journal of neuroscience methods*.
580 2011;198(1):84-92.

581 Tenan MS, Marti CN, Griffin L. Motor unit discharge rate is correlated within individuals: a case for
582 multilevel model statistical analysis. *J Electromyogr Kinesiol*. 2014;24(6):917-22.

583 Trajano GS, Orsatto LBR, McCombe PA, Rivlin W, Tang L, Henderson RD. Longitudinal changes in
584 intrinsic motoneuron excitability in amyotrophic lateral sclerosis are dependent on disease
585 progression. *J Physiol*. 2023;601(21):4723-35.

586 Trajano GS, Taylor JL, Orsatto LBR, McNulty CR, Blazeovich AJ. Passive muscle stretching reduces
587 estimates of persistent inward current strength in soleus motor units. *J Exp Biol*. 2020;223(Pt 21).

589 **Table 1.** Motor units' characteristics recorded during ramp contractions performed to 20% and 50% of maximal voluntary force in both control
 590 time points (i.e., CON-1 and CON-2). Data are presented as estimated marginal mean with 95% confidence intervals [CI].

	CON-1	CON-2	p value	
	ΔF score (Hz)	4.6 [4.0, 5.1]	4.8 [4.2, 5.3]	0.08
20%	Recruitment threshold (% MVC)	6.8 [5.6, 8.1]	6.2 [5.0, 7.4]	<0.001
	Derecruitment threshold (% MVC)	6.8 [6.0, 7.5]	7.0 [6.3, 7.8]	0.03
	Smoothed peak firing rate (Hz)	15.1 [14.1, 16.1]	15.0 [14.1, 16.0]	0.56
	ΔF score (Hz)	5.4 [4.7, 6.1]	5.4 [4.7, 6.1]	0.80
50%	Recruitment threshold (% MVC)	23.6 [19.6, 27.5]	24.6 [20.7, 28.6]	<0.001
	Derecruitment threshold (% MVC)	24.4 [20.7, 28.2]	25.6 [21.9, 29.3]	<0.001
	Smoothed peak firing rate (Hz)	20.2 [18.9, 21.6]	19.8 [18.4, 21.1]	<0.001

592 **CAPTIONS TO ILLUSTRATIONS**

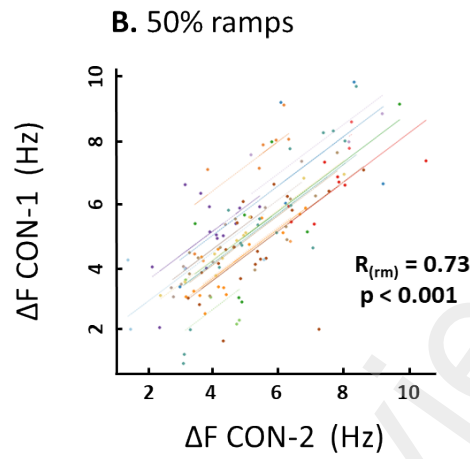
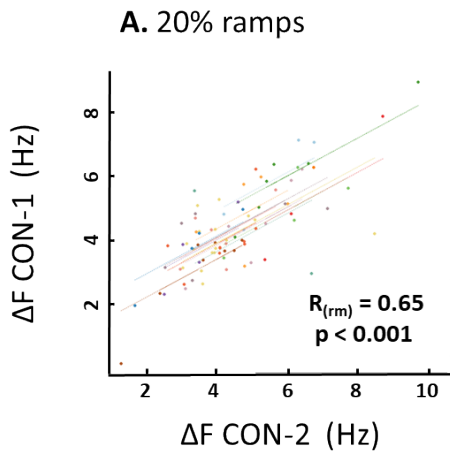
593

594 **Figure 1. Repeated-measures correlation ($R_{(rm)}$) plots illustrating the association between**
595 **ΔF scores in both CON-1 and CON-2.** Left panel (A) shows data from ramp contractions
596 performed to 20% of maximal voluntary contraction (MVC) torque and right panel (B) shows
597 data from ramp contractions performed to 50% MVC. Each colour represents a single
598 participant and parallel lines are fitted to test units from each participant. ΔF scores present a
599 large correlation between time points in the 20% MVC ramps, and a very large correlation in
600 the 50% MVC ramps.

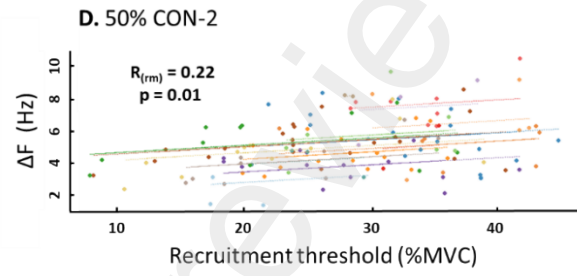
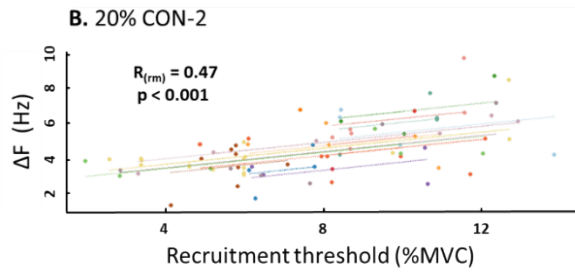
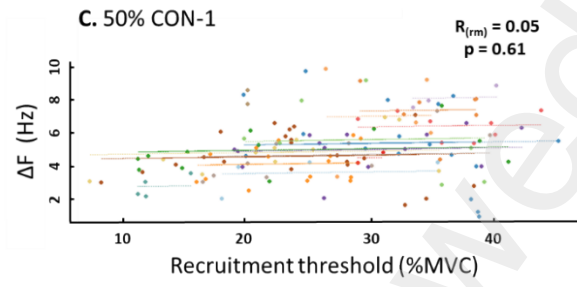
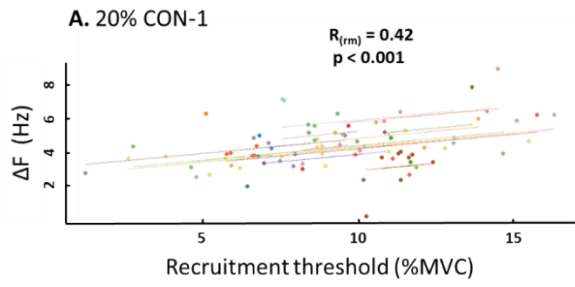
601

602 **Figure 2. Repeated-measures correlation ($R_{(rm)}$) plots illustrating the association between**
603 **recruitment threshold of test units and ΔF values.** CON-1 is presented in panels A and B.
604 CON-2 is presented in panels B and D. Values during ramp contractions performed to 20% of
605 maximal voluntary contraction (MVC) are presented in panels A and B. Values during ramp
606 contractions to 50% MVC are presented in panels C and D. Each colour represents a single
607 participant and parallel lines are fitted to test units from each participant. Except for 50% MVC
608 ramps in CON-1, weak to moderate positive correlations were observed, suggesting greater ΔF
609 scores in test units with higher recruitment-thresholds.

610



611



612